SAILING THE SARGASSO SEA FOR A FLOATING GOLDEN FOREST: THE APPLICATION OF GENETIC MARKERS TO INVESTIGATING *SARGASSUM* DIVERSITY AND DISTRIBUTION IN THE FIELD

By

Dani Hanelin

A Paper Presented to the

Faculty of Mount Holyoke College in

Partial Fulfillment of the Requirements for

the Degree of Bachelors of Arts with

Honor

Department of Biological Sciences

South Hadley, MA 01075

May 2019

This paper was prepared
under the direction of
Professor Renae Brodie
for eight credits.

ACKNOWLEDGEMENTS

I would first like to thank my thesis advisor, Renae Brodie, for the ongoing guidance, support, and encouragement with this year-long project. Renae's enthusiasm and desire to engage in conversations outside of my thesis kept me motivated to bring my best every week. I would also like to thank Dr. Kerry Whittaker and Sea Education Association (SEA) for the opportunity to continue, expand, and develop into an honors thesis the research that I began in Woods Hole, MA. For all things populations genetics at Mount Holyoke– the lab, equipment, and knowledge– I'd like to thank Jason Andras. For the funding that made this project possible, I'd like to thank the Mount Holyoke College Department of Biological Sciences and SEA. Lastly, I like to thank Jenny Renee and Alena Anderson, who put in countless hours scraping epibionts off *Sargassum*, extracting DNA at sea, and helping me begin this project abroad.

TABLE OF CONTENTS

LIST OF FIGURES

Page

ABSTRACT

Biodiversity and life in the oligotrophic Sargasso Sea are sustained by the free-floating macroalgae, Sargassum. Consisting of two species, S. fluitans and S. natans, pelagic Sargassum provides food, nutrients, and habitat to a diverse array of marine organisms. These two species are classified further into genetically distinct morphological forms, with S. fluitans III, S. natans I, and S. natans VIII being the most common in the Western North Atlantic. Since 2011, pelagic Sargassum populations have been shifting, delivering the previously rare morphotype, S. natans VIII, to Caribbean beaches in unprecedented quantities. These inundation events are detrimental to local fisheries, tourism, and coastal ecosystems. Developing efficient and cost-effective genetic tools to differentiate the three forms is imperative for studying morphotype distribution and the forces driving Caribbean inundation events. In our field-based study, we designed novel genetic primers to target two regions of the Sargassum mitochondrial genome, the cytochrome oxidase subunit 3 (Cox3) and NADH dehydrogenase subunit 6 (Nad6) to assess their efficacy to function as genetic markers. Both primers successfully differentiated the three morphotypes with varying accuracies (~89% for Cox3 and ~69% for Nad6) but have limitations in their applications. We also examined morphotype distribution patterns and found the highest concentrations of Sargassum in the Antilles Current and South Sargasso Sea, and overall density in both regions was comprised primarily of S. natans I and S. fluitans III. An examination of algal growth data indicated that S. natans VIII was older than other forms, which supports the hypothesis of a new Sargassum growth region in the tropics fueling inundation events.

INTRODUCTION

Since 2011, *Sargassum*, a holopelagic yellow-brown macroalgae, has been recurrently inundating Caribbean shores. These inundation events, also called "golden tides," result in large accumulations of *Sargassum* that engulf beaches and coasts, threatening local economies, tourism, fisheries, harbors, turtle nesting, and biodiversity (Maurer et al. 2015). The first major inundation event occurred during 2011-2012, the second during 2014-2015, and the most recent again in 2018, signaling to scientists and coastal communities alike that *Sargassum* distribution patterns were shifting. Historically, *Sargassum*, with its characteristic primarily oxygen-filled pneumatocysts, has been found floating between 20°N and 40°N latitude and from the Gulf Stream to 30°W longitude, with its highest concentrations suspended throughout the center of the North Atlantic Subtropical Gyre in a region called the Sargasso Sea (Parr 1939, Dooley 1972, Butler et al. 1983, Butler and Stoner 1984, South Atlantic Fishery Management Council 1998). The Sargasso Sea, unlike any other sea on Earth, is not defined by coastlines but by the currents that form the gyre: the Gulf Stream and Azores Current to the north, the Canary Current to the east, and the Antilles and North Equatorial Currents to the south. Because these currents are so dynamic and *Sargassum* is native to this region, several boundaries of the Sargasso Sea have been suggested, typically using a combination of oceanic circulation and *Sargassum* distribution to draw the lines (Ryther 1956, Butler et al. 1983, Coston-Clements et al. 1991). The most recent and comprehensive delineation of the Sargasso Sea, which was created for international conservation and management applications, offers a model that excludes all exclusive economic zones (EEZs) except Bermuda's and considers not only historical *Sargassum* distribution but

also physical, biological, and chemical oceanographic characteristics (Figure 1, Ardron et al. 2011, unpublished). This model was proposed by the Sargasso Sea Alliance and since then adopted in the Sargasso Sea Commission's latest management report, encompassing approximately 4,163,499 km^2 of ocean waters for international protection (Laffoley et al. 2011).

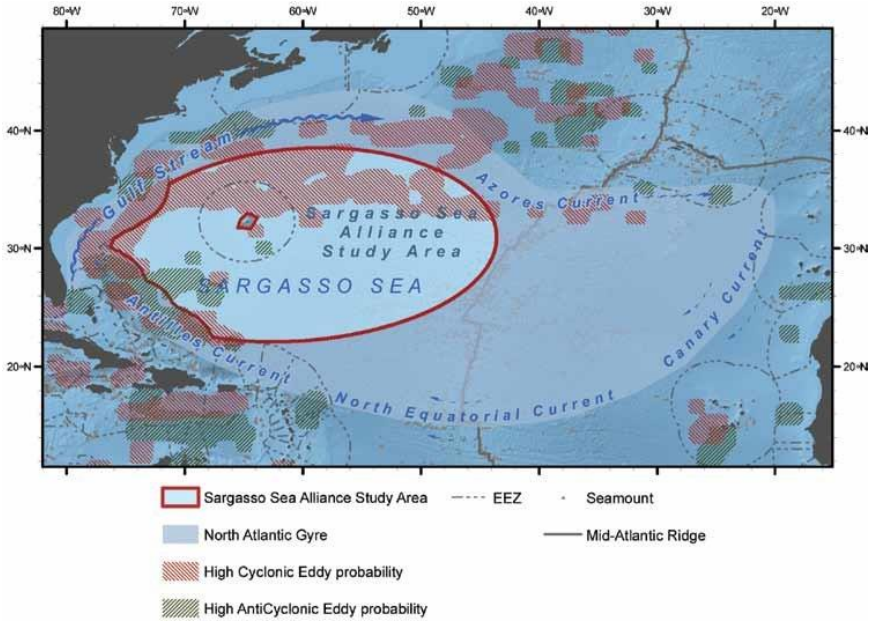

Figure 1. Boundaries of the Sargasso Sea defined by the Sargasso Sea Alliance for international management and conservation (Ardron et al. 2011, unpublished).

Although pelagic *Sargassum* only accounts for a small portion of the total primary production in the North Atlantic, it forms, in the otherwise oligotrophic waters of the Sargasso Sea, an essential structural habitat and spawning ground for a diversity of marine life. These habitats range in size from fist-sized, scattered clumps to wide mats or long windrows (Figure 2) that can form assemblages stretching over 100 miles (Carr 1987). Over 145 invertebrate species and 127 fish species, both adult and juvenile, seek habitat or refuge within while also providing nutrients for *Sargassum* (Butler et al. 1983, Coston-Clements et al. 1991, Lapointe 1995). Several commercially important species, including the white marlin (*Tetrapturus albidus*), blue

marlin (*Makaira nigricans*), American eel (*Anguilla rostrata)*, and European eel (*Anguilla anguilla*), spawn in *Sargassum*, while several endangered or critically endangered turtle species, including green turtles (*Chelonia mydas*), loggerhead turtles (*Caretta caretta*), hawksbill turtles (*Eretmochelys imbricate*), and Kemp's Ridley turtles (*Lepidochelys kempii*), use pelagic *Sargassum* as a nursery habitat during their "lost years," the nearly decade of time after a turtle hatches and travels out to sea before returning to coastal waters as a large juvenile (Carr 1987, Schwartz 1988, Manzella et al. 2011, South Atlantic Fishery Management Council 2002, Luckhurst et al. 2006, Bolden et al. 2007). Additionally, there are 10 known endemic species to pelagic *Sargassum*: the sargassum swimming crab *(Planes minutes*), sargassum shrimp (*Latreutes fucorum*), sargassum nudibranch (*Scyllea pelagica*), sargassum frogfish (*Histrio histrio*), sargassum pipefish (*Syngnathus pelagicus*), sargassum anemone (*Anemonia sargassensis*), sargassum snail (*Litiopa melanostoma*), a marine flatworm *Hoploplana grubei*, and two amphipods, *Sunampithoe pelagica* and *Biancolina brassicacephala* (Dooley 1972, Coston-Clements et al.1991).

Figure 2. A *Sargassum* windrow, formed by Langmuir circulations, seen in the South Sargasso Sea on April 27, 2018.

Given the uniqueness of these rich floating habitats, the extent and patterns of *Sargassum* distribution have fascinated scientists since the early 1930s. The first major attempts at quantifying *Sargassum* abundance and distribution involved a two-year study from 1933 to 1935 and a four-year study, several decades later, from 1977-1981 (Parr 1939, Stoner 1983). Stoner sampled along a similar route as Parr and found a significant decrease in *Sargassum* biomass over the approximately 40-year period (Stoner 1983). He speculated that the forces driving this decrease likely had anthropogenic roots, such as increased levels of pollutants in the ocean. However, another estimation in 1984 suggests that there was no overall significant decrease in biomass and Stoner's observations were likely a result of natural variation (Butler and Stoner 1984).

The recent Caribbean inundation events has sparked a particular interest in mapping large-scale *Sargassum* seasonal distribution and origins. Because satellites can detect floating vegetation with infrared light on a more global scale, many researchers have turned to remote sensing to create models and algorithms for *Sargassum* distribution and growth (Gower and King 2011, Gower et al. 2013, Johnson et al. 2013, Franks et al. 2016, Wang and Hu 2016, Brooks et al. 2018, 2019). Gower and King (2011) used satellite imagery data (2002-2008) from the European Space Agency (ESA) Medium Resolution Imaging Spectrometer (MERIS) optical sensor and made the first map of *Sargassum* distribution in the Gulf of Mexico and Western North Atlantic. They identified a *Sargassum* source region in the Northwest Gulf of Mexico in which the algae grow annually between March and June until advection carries it to the Atlantic beginning in July (Gower and King 2011).

Since the 2011 inundation event, other studies have identified a new *Sargassum* source region considerably farther south (Gower et al. 2013, Johnson et al. 2013, Franks et al. 2016, Putnam et al. 2018, Brooks et al. 2018). Johnson et al. (2013), using a backtracking model, suggested that the *Sargassum* associated with the 2011 inundation event originated in the North Equatorial Recirculation Region (NERR). Other researchers, using synthetic particle tracking experiments, have additionally identified the North Brazil Current System (NBCS) as central in transporting *Sargassum* from the equatorial Atlantic to the Caribbean during inundation events (Putman et al. 2018). Similarly, Franks et al. (2016) found *Sargassum* transport pathways from the Western Tropical Atlantic to the Caribbean, and Brooks et al. (2018), in addition to the western Gulf of Mexico, likewise found that the Western Tropical Atlantic is responsible for fostering seasonal *Sargassum* growth.

While this new two-source hypothesis is well-supported, there is debate in whether a return pathway for *Sargassum* exists from the Sargasso Sea back to tropics. Modeling by both Johnson et al. (2013) and Franks et al. (2016) suggested that *Sargassum* is unable to return to these equatorial regions. A new model, however, suggests that inertia can increase *Sargassum* transport up to 20%, enough to create a return pathway to the tropics from the Sargasso, but no additional work has confirmed this hypothesis (Brooks et al. 2019).

Other researchers have used remote sensors to quantify and predict *Sargassum* distribution overtime. Wang and Hu (2016) used the Moderate Resolution Imaging Spectroradiometer (MODIS) to conduct a hindcast analysis of *Sargassum* abundance observations from 2000-2016 and revealed that *Sargassum* coverage patterns began increasing starting in 2011 and were significantly higher than ever before in 2014- 2015. A year later, Wang and Hu (2017) developed probability maps capable of predicting blooms with over 80% accuracy. While it remains an invaluable tool, satellite technology does not encapsulate a comprehensive story of *Sargassum* distribution. It leaves out patterns and composition at a species level, something only field sampling can explain.

Pelagic *Sargassum* consists of two species, *Sargassum fluitans* and *Sargassum natans*. Setting them apart from other seaweeds, both species are sterile and reproduce solely by vegetative fragmentation (Butler et al. 1983). As uncovered by Parr's fieldwork in the 1930s, within each species, there are distinct morphological forms, or morphotypes: *S. natans I, II, VIII, IX* and *S. fluitans III, X*, with *S. natans I* and *S. fluitans III* being most abundant (Parr 1939). Currently, the three most common morphotypes in the Western North Atlantic, and those targeted for this study, are *S. fluitans III*, *S. natans I,* and the previously rare *S. natans VIII* (Figure 3).

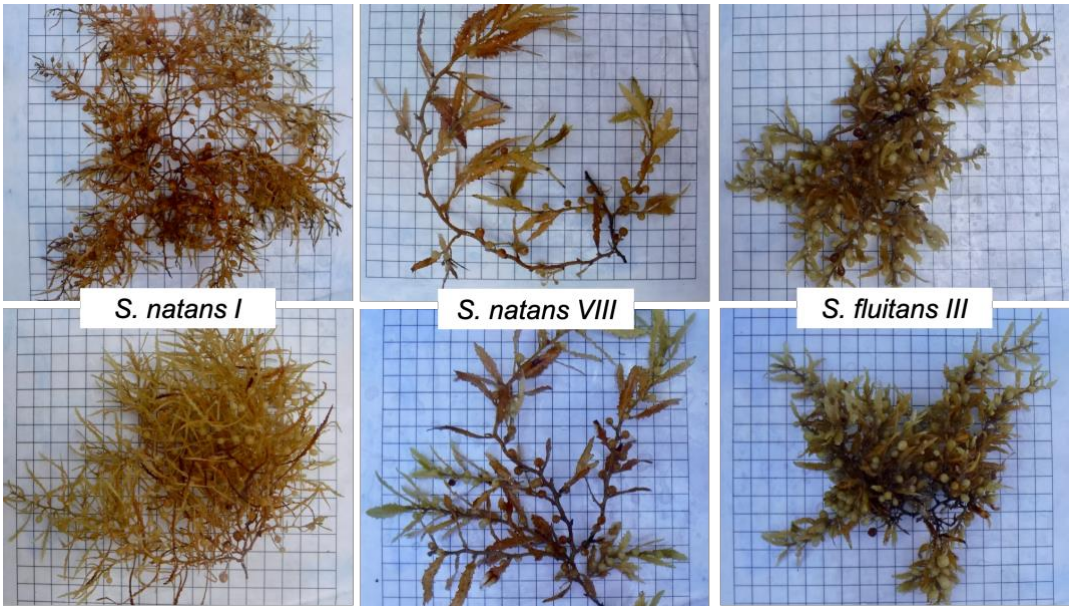

Figure 3. The three most common pelagic *Sargassum* morphotypes in the Western North Atlantic, *S. natans I*, *S. natans VIII*, and *S. fluitans III*.

Parr's (1939) patterns of morphotype relative abundance held true until recently when Schell et al. (2015), in response to the 2014 and 2015 Caribbean inundation events, found from field observations that concentrations of *S. natans VIII* were the highest that they had been in about 20 years throughout the Antilles Current, Eastern Caribbean, and Western Tropical Atlantic. Schell et. al (2015) found that *S. natans VIII* dominated the tropics, while *S. fluitans III* dominated the South Sargasso Sea. Additionally, Amaral-Zettler et al. (2016) identified *S. natans VIII* as the morphotype responsible for the Caribbean inundation events. These findings are consistent with the two-source hypothesis, but more importantly they add clarity by identifying exactly which morphotype is growing in the Western Tropical Atlantic and inundating the Caribbean.

The culmination of all current satellite, field, and genetic research emphasizes three important points: 1) *Sargassum* distribution and populations shifting even at a morphotype-level, 2) a new *Sargassum* source region exists, fueling inundation events and delivering a previously

rare morphotype to the Caribbean in unprecedented amounts, and 3) a comprehensive understanding of *Sargassum* distribution necessitates a combination of satellite technology and field observations. In order to accomplish the latter and make accurate *Sargassum* morphotype identifications in the field, we must develop efficient and cost-effective methods for differentiating the three forms. Genetic tools are the most useful because morphological identifications of *Sargassum* morphotypes can be both subjective and challenging, due in part to the similarities between *S. fluitans III* and *S. natans VIII,* discrepancies in the literature regarding differentiating morphological features, as well as the ambiguity and variability in morphological traits (Amaral-Zettler et al. 2016, Figure 4)

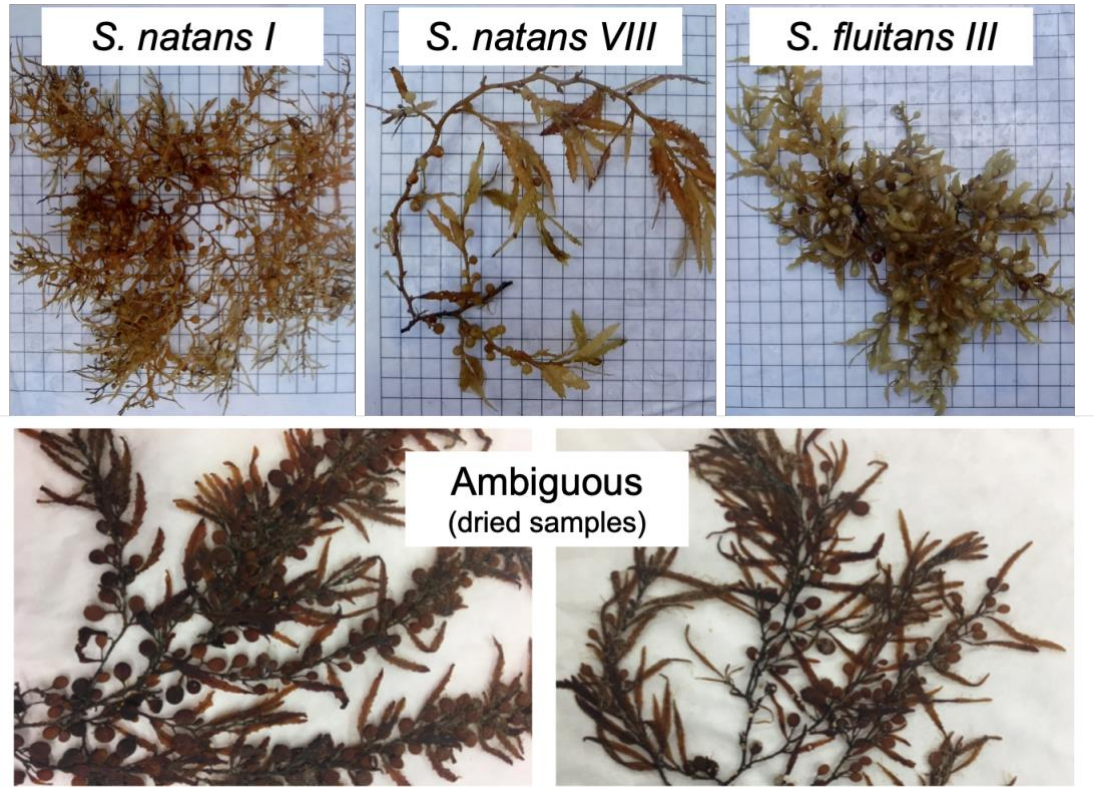

Figure 4. Morphologically ambiguous dried specimens from the North Sargasso Sea (bottom) against the three morphotypes (top).

Genetic analyses of pelagic *Sargassum* is a recent development in the field of molecular ecology. In fact, up until 2016, scientists were still unsure whether the three morphotypes were

even genetically distinct. When Amaral-Zettler et al. (2016) generated full mitochondrial genomes and partial chloroplast genomes of *S. fluitans III*, *S. natans I,* and *S. natans VIII*, they found that all three were genetically distinct, and for the first time ever we had molecular confirmation of Parr's findings from the 1930s. Specifically, the authors found consistent sequence differences between *S. natans I* and *VIII* (seven base pairs out of 34,727) as well as a close phylogenetic relationship between *S. fluitans III* and *S. natans I* and *VIII* (Amaral-Zettler et al. 2016). In the mitogenome of *S. natans I* and *VIII*, Amaral-Zettler et al. (2016) found single nucleotide polymorphisms (SNPs) in five protein-coding genes: ribosomal protein L5 (rpl5), ribosomal protein S19 (rps19), ribosomal protein S13 (rps13), cytochrome oxidase subunit 3 (Cox3), and NADH dehydrogenase subunit 6 (Nad6). Genetic tools have the potential to enhance field-based questions, such as those about sub-taxonomic *Sargassum* diversity, abundance, and distribution over time, by confirming morphological identifications. In particular, genetic markers that can delineate the morphotypes are especially useful because they provide molecularly supported data at a cost much lower than sequencing the entire genome.

In this study, we designed novel molecular primers to amplify the two mitochondrial regions identified by Amaral-Zettler et al. (2016), Cox3 and Nad6, to investigate (1) how effectively these markers could differentiate the three morphotypes and (2) how patterns of *Sargassum* distribution compared across morphotypes and regions– the Antilles Current, South Sargasso, and North Sargasso. Our study is the first to use molecular data to address questions of *Sargassum* morphotype distribution in the field. Our work will help further develop the pelagic *Sargassum* genetic toolkit and provide an update on morphotype distribution since Schell et al. (2015). With evidence of recent shifts in *Sargassum* distribution and a new source region delivering a previously rare form to the Caribbean, it remains imperative that we develop

accurate and cost-effective molecular tools that can differentiate the three morphotypes so scientists and coastal communities have a means to monitor *Sargassum* distribution and address questions regarding inundation events.

METHODS

Field Sampling

Sargassum samples were collected at 47 stations during a Sea Education Association (SEA, Woods Hole, Massachusetts, USA) research cruise (C279, 2018) through the Antilles Region, Sargasso Sea, and North Atlantic Ocean from April 18 to May 24, 2018 (Figure 5).

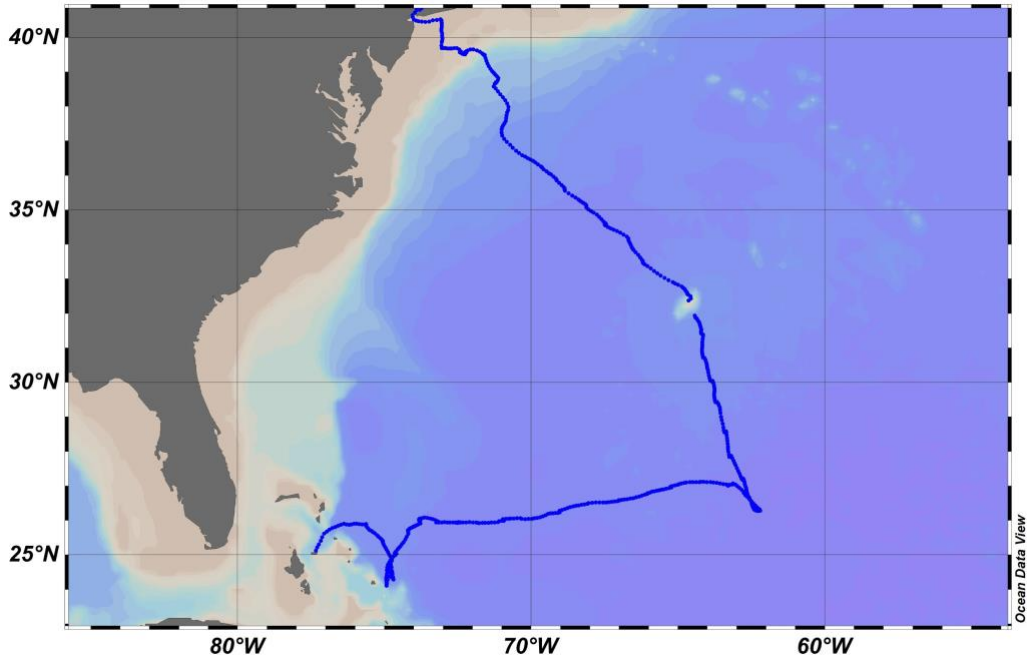

Figure 5. Sea Education Association (SEA, C-279) cruise track from Nassau, Bahamas to St. George's, Bermuda and New York City, NY.

During daily morning stations at approximately 0900, we used a 333.0 µm mesh dip-net to collect *Sargassum*, with the intent of collecting at least one sample for each of the three forms (*S. natans I, S. natans VIII, and S. fluitans III*) and one form per dip-net in isolated clumps or fragments. We used opportunistic dip-net sampling in order to maximize the number of samples of each morphotype for genetic marker testing. In addition, we collected *Sargassum* samples via Neuston tows (1.0 m wide × 0.5 m high, 333 µm mesh net), which were deployed twice per day

at approximately 1130 and 2300, for a total of 41 tows (Figure 6). The net was towed over the surface at approximately two knots for 20 or 30 minutes, with a goal of maintaining an average height of the surface water line at the center of the net opening. For all sampling techniques, *Sargassum* clumps were assigned a morphotype identification using the morphological attributes established by Parr (1939) and those used in morphotype distribution analyses were later confirmed with molecular techniques.

Figure 6. Neuston tow sampling of *Sargassum* from the SSV *Corwith Cramer*.

Molecular Analysis

A 5-10 cm piece of the newest growth was clipped from each *Sargassum* sample, scraped clean of epibionts, and then placed in silica desiccant for at least 48 hours. Once sufficiently dried, 3-4 dried leaves were ground into a homogenized powder with a disposable pellet pestle in a 2 ml microcentrifuge tube to begin the extraction process. Deoxyribonucleic acid (DNA) was extracted with the MoBio DNeasy Power Plant Pro Kit (Carlsbad, CA, USA) and a modified version of the manufacturer protocol was used. This method mirrored Wilson et al. (2016) to replace the step of bead beating and an extra 24-hour incubation period. The extracted DNA was purified according to manufacturer protocols with the MoBio DNeasy Power Clean Pro Kit (Qiagen Ltd., Crawley, UK).

The Cox3 mitochondrial gene was targeted using novel primers (Cox3KAWF: 5'-TCGAATCCTATCCCCTTCTTAA-3' and Cox3KAWR: 5'-GGCCAAACCCCTCCAATATTAC-3'). The NADH dehydrogenase subunit 6 (Nad6) region was also targeted using novel primers (SargNad6F: 5'-TATGATTCTTGGGGCTGGT-3' and SargNad6R: 5'-GGGATCATTCAAAGCAGAAGA-3'). Samples that did not initially yield high quality double-stranded Nad6 sequences, were re-sequenced using internal primers (Nad6IntF: 5'- NAD6TACGGTTTTTATAGGAASTTCCTATG- 3' and Nad6IntR: 5'-CTGTTTTTGCCCAGAAGACCA- 3'). Both the Cox3 and Nad6 markers were polymerase chain reaction (PCR) amplified from DNA in 50 L reactions composed of 18µL of molecular-grade water, 10 µM of the forward primer, 10 µM of the reverse primer, 1µL of Bovine Serum Albumin (BSA) (New England Biolabs, Ipswich, MA, USA), 25 µL of OneTaq Hot Start 2X Master Mix with Standard Buffer (New England Biolabs, Ipswich, MA, USA), and 2 µL of DNA.

PCR amplification was performed on the Bio-Rad thermocycler (Hercules, CA, USA). PCR protocols varied depending on the marker being amplified (Appendix Table 1, 2). PCR products were verified with agarose gel electrophoresis and purified with the Qiagen Qiaquick PCR Cleanup Kit (Qiagen Ltd., Crawley, UK). The purified PCR product was then profiled with a Nanodrop ND-1000 Spectrophotometer to examine the purity and concentration of the DNA. The purified PCR products were sequenced by the DNA Analysis Facility on Science Hill (New Haven, CT) in both directions with the forward and reverse primers from the amplification step. For the samples we re-sequenced, the Nad6 forward and reverse internal primers were also used for sequencing.

A total of 57 Cox3 sequences and 43 Nad6 sequences were analyzed and sent to GeneBank. The two individual loci were aligned, manually corrected, and analyzed in Geneious Prime (v.11.1.4). Maximum likelihood (ML) trees were generated based on a Hasegawa-Kishino-Yano (HKY) substitution model using PhyML v.3.3 (Dufayard et al. 2010) and rooted using *Sargassum vachellanium* as the outgroup. A known sample for each morphotype from GeneBank was also used to generate trees, each labeled with their GeneBank ID. The node support for the ML analyses were based on 1000 bootstrap iterations.

Distribution Analysis

Sargassum samples, for the purpose of regional analyses, were grouped into three general locales: Antilles Current, South Sargasso, and North Sargasso (Figure 7). All statistical analyses were conducted using JMP® (version 14, SAS Institute Inc., Cary, NC, 1989-2019).

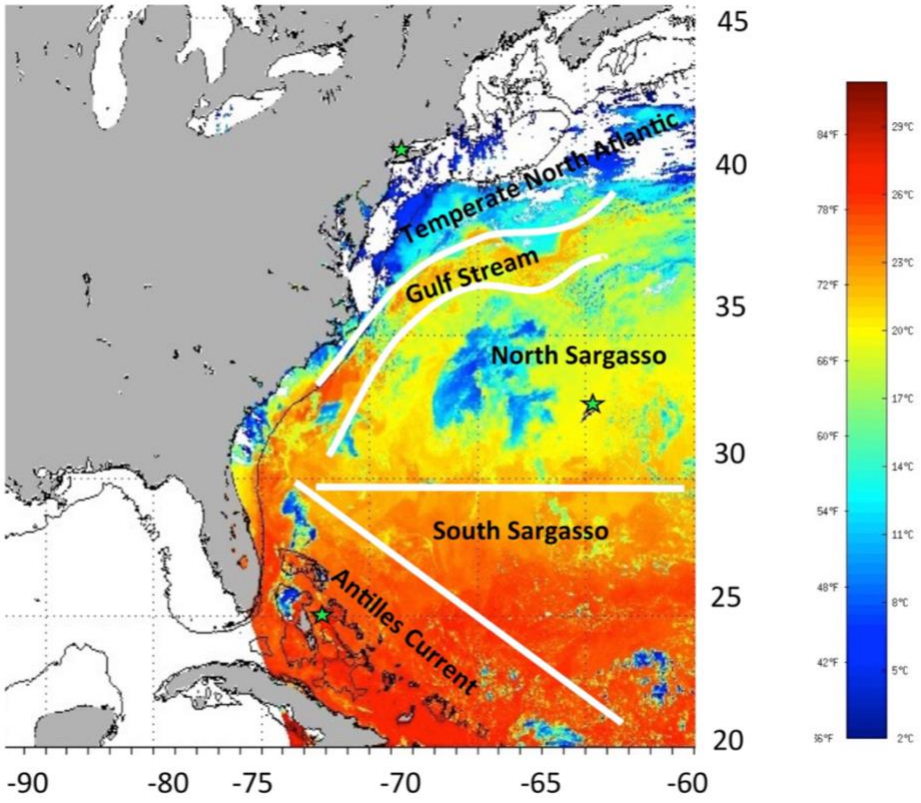

Figure 7. General locale map indicating the study regions (Antilles Current, South Sargasso, and North Sargasso) and sea surface temperature from April 14, 2018.

A two-way ANOVA of morphotype and locale on average *Sargassum* density with a square root transformation to correct for zeroes was used to assess the impact of morphological form and region on overall density. A one-way ANOVA of morphotype on *Sargassum* new growth was used to evaluate the effect of morphological form on *Sargassum* growth. Both analyses were followed by a post-hoc t-test for pairwise comparisons. *Sargassum* distribution data was obtained from samples collected via Neuston tows (n=28, excluding 13 tows from the

Hudson Canyon and Gulf Stream regions) to avoid the bias associated with opportunistic dip-net sampling. The one exception to this rule was with *Sargassum* new growth percentages, as this data was only collected with dip-net sampling. After each Neuston tow, *Sargassum* mass was measured using a scale for each clump obtained and density was calculated using the tow distance. *Sargassum* samples collected via opportunistic dip-net sampling were recorded for their new growth percentages, using Munsell Charts and algal coloration. Other basic environmental (e.g. atmospheric temperature, wind direction, cloud cover) and oceanographic data (e.g. sea surface temperature, salinity, fluorescence) were collected along tows, at stations, and continuously along the cruise for SEA's long-term database. SEA, in addition, saved a 4-5 cm frond of each *Sargassum* sample in ethanol as morphological vouchers for its biological collection.

RESULTS

Cox3 and Nad6 Markers

Both markers were capable of grouping the three morphotypes into distinct clades on a maximum likelihood (ML) phylogenetic tree, but the clades for were not well-supported, bootstrap values <70.0 (Figure 8a, 9a). The Cox3 marker had two informative single nucleotide polymorphisms (SNPs) at BP81 and BP131 (Figure 8b). Overall marker efficacy (i.e. when a genetic identity matched the morphological identification) for the Cox3 marker was 89.09% (49/55). Marker accuracy for individual morphotypes was higher: 95.45% for *S. fluitans III*, 100% for *S. natans I*, and 100% for *S. natans VIII* (Figure 8b). There was only one case in which the genetic identity was inconsistent with the morphological identity (1/55), but five cases (5/55) with ambiguous genetic codes (R= A or G) at one or both informative SNPs (Figure 8b). These five cases were labeled as "unconfirmed" on the tree and associated table– while we did have a morphological identity, we could not confirm a genetic identity with this marker (Figure 8). Also, for an evaluation separate of marker efficacy, we included two additional samples that exhibited ambiguous morphology in our tree, indicated by stars (Figure 8).

a.

b.

	BP81	BP131	Cox3 ID	n	Accuracy
S. fluitans III	A	G	sf3	22	95.45%
S. natans I	G	A	sn1	19	100%
S. natans VIII	G	G	sn8	9	100%
Unconfirmed	R	G	unconfirmed	2	
	R	R	unconfirmed	3	
Misidentified				1	
Overall Cox3 Efficacy	49/55		**89.09%**		

Figure 8 a. Maximum likelihood evolutionary relationship generated using the Cox3 marker (Hasegawa-Kishono-Yano substitution model; 1000 bootstrap replicates for node support). Samples with unconfirmed molecular identities are indicated as such with morphological (morph) and Nad6 marker identities in parentheses. Stars indicate samples with ambiguous morphology and were not included in the marker efficacy analysis **b.** Informative SNPs and marker efficacy table.

The Nad6 marker, on the other hand, had three informative SNPs at BP56, BP177, and BP196, and an overall efficacy of 69.05% (29/42) (Figure 9). Nad6 marker accuracy for individual morphotypes was 76.47% for *S. fluitans III*, 84.62% for *S. natans I*, and 62.50% for *S. natans VIII* (Figure 9b). There were nine cases in which the genetic ID was inconsistent with the morphological ID (9/42) and four cases (4/42) with low-frequency sequence variance (Figure 9b). These four cases were labeled "unconfirmed" on the tree and associated table– while we did have a morphological identification, we could not confirm a genetic identity with this marker (Figure 9). Once again, for an evaluation separate of marker efficacy, we included one additional sample in our tree that exhibited ambiguous morphology, indicated by a star (Figure 9).

a.

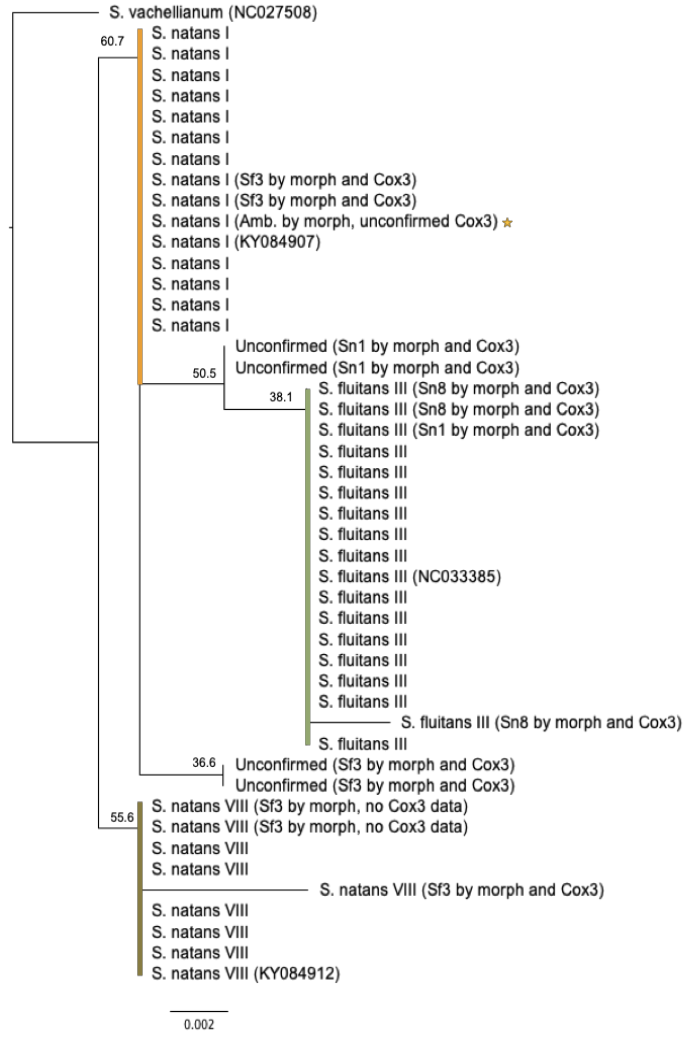

b.

	BP56	BP177	BP196	Nad6 ID	n	Accuracy
S. fluitans III	G	T	C	sf3	17	76.47%
S. natans I	A	T	G	sn1	13	84.62%
S. natans VIII	A	A	G	sn8	8	62.50%
Unconfirmed	A	T	C	unconfirmed	2	
	G	T	G	unconfirmed	2	
Misidentified					9	
Overall Nad6 Efficacy	29/42			**69.05%**		

Figure 9 a. Maximum likelihood evolutionary relationship generated using the Nad6 marker. (Hasegawa-Kishono-Yano substitution model; 1000 bootstrap replicates for node support). Samples with unconfirmed molecular identities are indicated as such with morphological (morph) and Cox3 marker identities in parentheses. Stars indicate samples with ambiguous morphology and were not included in the marker efficacy analysis **b.** Informative SNPs and marker efficacy table.

Sargassum Distribution

Sargassum density varied by morphotype and location, with highest densities in the South Sargasso and Antilles regions and *S. natans I* and *S. fluitans III* being the most abundant morphotypes. General locale, species (morphotype), and the interaction effect of locale and species were all significant predictors of *Sargassum* density (Figure 10a; $F_{2,102}$=15.707, $F_{2,102}$=13.350, $F_{4,102}$=4.114, $p<0.05$ respectively). Starting with locale independent of morphotype, overall average *Sargassum* density was highest in the South Sargasso (0.10 ± 0.01 gm^{-2}), followed by the Antilles (0.05 ± 0.03 gm^{-2}), while lowest in the North Sargasso ($0.01 \pm 0.02 gm^{-2}$) (Figure 10b). Overall *Sargassum* density was significantly lower in the North Sargasso Sea than in both the South Sargasso and Antilles ($p<0.05$), while overall *Sargassum* density was not significantly different between the Antilles and South Sargasso ($p>0.05$). Considering species independent of locale, *S. natans I* accounted for the highest average density (0.11 ± 0.02 gm^{-2}), followed by *S. fluitans III* (0.07 ± 0.02 gm^{-2}), while *S. natans VIII* accounted for the lowest density (0.002 ± 0.02 gm^{-2}) (Figure 10c). The average density of *S. natans VIII* was significantly lower than that of both *S. fluitans III* and *S. natans I* ($p<0.05$), while there was no significant difference between the densities of latter two morphotypes (Figure 10c, $p>0.05$). Considering the combination of locale and morphotype, *S. natans I* in the South Sargasso accounted for the highest density ($0.187 \pm 0.049 gm^{-2}$), followed by *S. natans I* in the Antilles (0.112 ± 0.039 gm^{-2}), *S. fluitans III* in the South Sargasso (0.109 ± 0.028 gm^{-2}), *S. fluitans III* in the Antilles (0.024 ± 0.009 gm^{-2}), *S. fluitans III* in North Sargasso (0.018 ± 0.007 gm^{-2}), *S. natans I* in the North Sargasso (0.005 ± 0.003 gm^{-2}), *S. natans VIII* in the Antilles (0.005 ± 0.002 gm^{-2}), *S. natans VIII* in the South Sargasso (0.002 ± 0.001 gm^{-2}), and *S. natans VIII* in the North Sargasso (0.0001 ± 0.0001 gm^{-2}) (Figure 10a). Within sites, there

were three cases in which *Sargassum* densities were significantly different between morphotypes (Figure 10a, $p<0.05$).

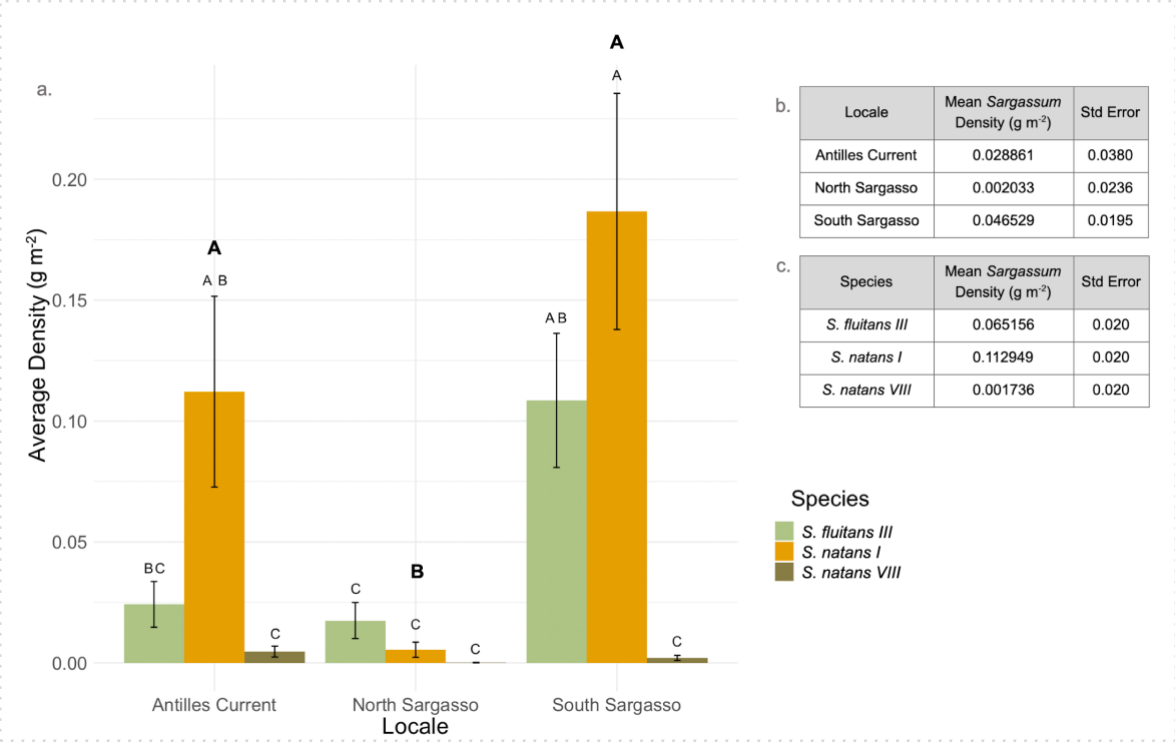

Figure 10. Average *Sargassum* density (gm^{-2}) and standard error by morphotype in the Antilles, North Sargasso, and South Sargasso regions from Neuston tow sampling ($F_{8,102}=11.291$, $p<0.05$) Actual values are reported in the figure, but all statistical analyses were conducted using a square root transformation. Post-hoc t-tests, indicated by letters, were conducted for group differences within (non-bold) and across (bolded) the three general locales, where different letters represent a significant difference ($p<0.05$).

Lastly, for *Sargassum* clumps collected via dip-net sampling, the average new growth– an indicator of sample age– was highest in *S. natans I* samples (0.516 ± 0.04), followed by *S. fluitans III* (0.381 ± 0.03), while lowest in *S. natans VIII* (0.260 ± 0.102) (Figure 11). Species was a significant indicator of average new growth ($F_{2,96}=5.542$, $p<0.05$). New growth of *S. natans I* was significantly different from that of both *S. fluitans III* and *S. natans VIII* ($p<0.05$), but there was no significant difference between new growth of *S. fluitans III* and *S. natans VIII* ($p>0.05$ Figure 11).

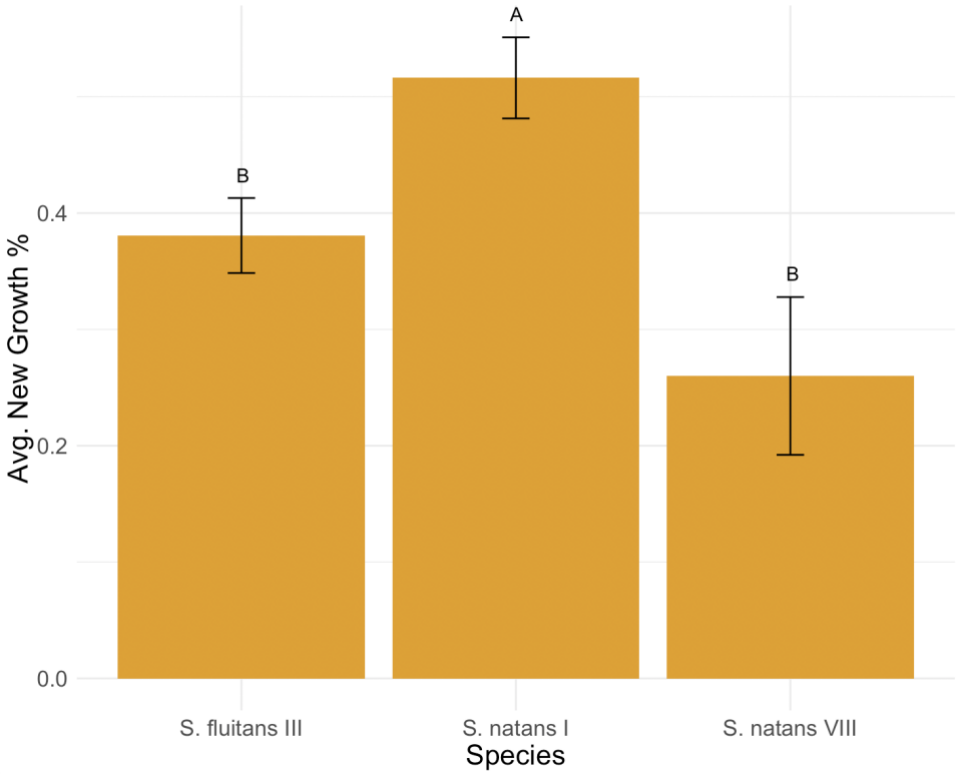

Figure 11. Average new growth percentage for *Sargassum* clumps collected via dep-net sampling ($F_{2,96}$=5.542, $p<0.05$). Post-hoc t-tests, represented by letters, were conducted for group differences, where different letters represent a significant difference ($p<0.05$).

DISCUSSION

As Caribbean inundation events have intensified in the past eight years, scientists and coastal communities have become increasingly more interested in monitoring and modeling pelagic *Sargassum* in the Western Atlantic. Molecular markers have the potential to serve as a simple, low-cost means to address species-specific questions of distribution, especially given the variability of morphological traits within the two pelagic *Sargassum* species. The novel genetic primers we developed for this study successfully differentiated the three most common morphotypes in the Western Atlantic, *S. fluitans III*, *S. natans I, S. natans VIII*, using variation in polymorphic sites across two mitochondrial genes, Cox3 and Nad6. Our phylogenetic analysis grouped the majority of sequences into three distinct clades, one for each of the three morphotypes (Figure 8, 9). The clades, however, were not well-supported (bootstrap values <70.0) for either marker, which limits the application of our primers. We would not suggest they be used for evolutionary analyses pertaining to questions of, for example, speciation or adaptive radiation of morphotypes. Though, we would strongly urge applying them to future field studies that help monitor and model patterns of *Sargassum* morphotype distribution. For the most part, our knowledge of pelagic *Sargassum* morphotype spatial ecology in the Western Atlantic remains minimal because researchers have lacked the tools to identify accurately the different morphotypes. Our work builds on the comparative mitochondrial analysis by Amaral-Zettler et al. (2016) and is a major step forward in developing a genetic toolkit for delineating inundation-associated *Sargassum* morphotypes and continuing to monitor their populations in the field.

Overall, the Cox3 marker, was a more effective tool than the Nad6 marker. When the Cox3 marker does make a molecular identity, it is 95.45-100% accurate, depending on the morphotype (Figure 8a). Occasional variants (5) exhibiting ambiguous genetic codes (R= A or G), as opposed to inaccurate molecular identities (1), decreased the overall efficacy of the marker (Figure 8a). The five samples with ambiguous genetic codes were most likely a result of sequencing error, rather than hybridization, because their morphological identifications were confirmed by the Nad6 marker when data was available (3/5 confirmed by the Nad6 marker; 2/5 had no available Nad6 data).

The Nad6 marker, on the other hand, had an accuracy range of 62.50-84.62%, with several (9) inaccurate molecular identities and (4) low-frequency sequence variants (Figure 9b). Because all four variant samples exhibited clear morphology confirmed by the Cox3 marker, it is unlikely that the variation is a result of hybridization. Due to the number of misidentified and variant samples with the Nad6 marker, we would suggest that the Cox3 marker be the first-choice tool. While we do propose that our primers, particularly the Cox3 primer, be applied to future field-based spatial ecology studies, we also acknowledge that the tool is imperfect and developing different sequencing tools would help with other research applications.

Because of the remarkable genetic similarity across *Sargassum* taxa, especially within species, single marker genes have their limitations with this organism. Future research could consider testing microsatellite markers, as they tend to be highly polymorphic and thus more appropriate for answering evolutionary questions (Freeland et al. 2012). Additionally, because we found no patterns with our samples exhibiting ambiguous morphology–labelled with a star on the phylogenetic trees (Figure 8, 9)– other more polymorphic sequencing tools, like microsatellite markers, may help resolve uncertainties with their identities.

Between the first recorded inundation event in 2011 and the most recent standings in 2018, many researchers have turned to remote sensing and distribution modeling to address the large-scale forces driving inundation events, such as a new *Sargassum* source region in the Western Tropical Atlantic (Gower et al. 2013, Johnson et al. 2013, Franks et al. 2016, Putnam et al. 2018, Brooks et al. 2018). Although few are published, field-based studies add a layer of specificity to satellite findings by describing species and morphotype patterns. Some of the oldest field work on pelagic *Sargassum* dates back to the 1930s when the morphotypes were first recognized. Parr (1939) found that *S. natans I* was and *S. fluitans III* were the most abundant forms in the Western North Atlantic, and the majority of *Sargassum* biomass was situated within the Sargasso Sea. Our relative abundances are consistent with Parr's findings: *S. natans I* and *S. fluitans III* accounted for the majority *Sargassum* density both regionally and overall, but unlike Parr, we found the majority of *Sargassum* within the Antilles and South Sargasso (Figure 10).

Our distribution findings are more consistent with the recent work of Schell et al. (2015), who found unprecedented quantities of *Sargassum* in regions south of the Sargasso. Like Schell et al. (2015), we found that *S. natans I* dominated the South Sargasso, but we did not find the same patterns of *S. natans VIII* in the Antilles as the 2015 researchers did (Figure 10). Our findings suggest that *S. natans VIII* remains relatively rare in that region, at least during the month of April. Gower and King (2011) found that *Sargassum* has annual growth blooms between the months of March and June in the Northwestern Gulf of Mexico, the first source region, while Gower et al. (2013) found the highest *Sargassum* detection counts during July and September in the Western Tropical Atlantic, the second source region. Therefore, because Schell et al. (2015) sampled in November and we sampled in April, it is possible that the different relative abundances we found in the Antilles was a result of seasonal variation.

Although relatively rare, when we did encounter *S. natans VIII*, it was typically in the form of small fragments and older than other forms. Since the first inundation event, researchers have identified and confirmed *S. natans VIII* as originating in the new source region and responsible for inundation events (Schell et al. 2015, Amaral-Zettler et al. 2016). Our new growth analysis showed that *S. natans VIII* was significantly older than our most abundant form, *S. natans I*, (Figure 11). A possible explanation for this finding, that remains consistent with the two-source hypothesis, is that the *S. natans VIII* we encountered originated in the new source region in the Western Tropical Atlantic, while other forms originated in the Northwest Gulf of Mexico. Seasonal variation may also be a factor, but this question just accentuates our need to continue studying *Sargassum* morphotype distribution, both spatially and temporally. Now that we have developed and applied genetic tools for field analyses of pelagic *Sargassum* morphotype distribution and ecology, we hope that other researchers and groups will use our findings to develop a long-term population monitoring plan that both furthers our understanding of the macroalgae and aids coastal communities in preparing and responding to inundation events.

LITERATURE CITED

Amaral-Zettler, L., N. Dragone B., J. Schell, B. Slikas, L. Murphy G., C. Morrall E. and E. Zettler. 2016. Comparative mitochondrial and chloroplast genomics of a genetically distinct form of Sargassum contributing to recent "Golden Tides" in the Western Atlantic. Ecol. Evol. **7:** , doi:10.1002/ece3.2630.

Ardron, J., P. Halpin, J. Roberts, J. Cleary, R. Moffitt and B. Donnelly. 2011. Where is the Sargasso Sea? A Report Submitted to the Sargasso Sea Alliance. Sargasso Sea Alliance Science Report Series. **24:** , doi:10.1163/15718085-12341399.

Bolden, S., R. Blankinship, K. Damon-Randall, J. Hoolihan, and S. Nichols. 2007. Atlantic

White Marlin Status Review. NMFS, Southeast Regional Office.

Brooks, M. T., V. J. Coles, R. R. Hood and J. Gower. 2018. Factors controlling the seasonal distribution of pelagic Sargassum. Mar. Ecol. Prog. Ser. **599:** 1-18, doi:10.3354/meps12646.

Brooks, M. T., V. J. Coles and W. C. Coles. 2019. Inertia Influences Pelagic Sargassum Advection and Distribution. Geophys. Res. Lett. **46:** 2610-2618, doi:10.1029/2018GL081489.

Butler, J. N., B. F. Morris, J. Cadwallader and A. Stoner. 1983. Studies of Sargassum and the Sargassum community. Bermuda Biological Station Special Publication. **22:** 1-307.

Butler, J. N. and A. W. Stoner. 1984. Pelagic Sargassum: has its biomass changed in the last 50 years? Deep Sea Research Part A. Oceanographic Research Papers. **31:** 1259-1264, doi://doi.org/10.1016/0198-0149(84)90061-X.

Carr, A. 1987. New Perspectives on the Pelagic Stage of Sea Turtle Development. Conserv. Biol. **1:** 103-121, doi:10.1111/j.1523-1739.1987.tb00020.x.

Coston-Clements, L., L. R. Settle, D. E. Hoss, and F. A. Cross. 1991. Utilization of the Sargassum habitat by marine invertebrates and vertebrates, a review. NOAA Technical Memorandum.

Dooley, J. 1972. Fishes associated with the pelagic Sargassum complex, with a discussion of the Sargassum community. Contrib. Mar. Sci. **16:** 1-32.

Dufayard, J. F., V. Lefort, M. Anisimova, W. Hordijk and O. Gascuel. 2010. New Algorithms and Methods to Estimate Maximum-Likelihood Phylogenies: Assessing the Performance of PhyML 3.0. Syst. Biol. **59:** 307-321.

Franks, J.,S., D. Johnson R. and D. Ko. 2016. Pelagic Sargassum in the Tropical North Atlantic. Gulf Caribb.Res. **27:** , doi:10.18785/gcr.2701.08.

Freeland, J. R., H. Kirk, and S. D. Peterson. 2012. Molecular Markers in Ecology, p. 35-75. *In* Anonymous Molecular Ecology. John Wiley & Sons, Ltd.

Gower, J. F. R. and S. A. King. 2011. Distribution of floating Sargassum in the Gulf of Mexico and the Atlantic Ocean mapped using MERIS. Int. J. Remote Sens. **32:** 1917-1929, doi:10.1080/01431161003639660.

Gower, J., E. Young and S. King. 2013. Satellite images suggest a new Sargassum source region in 2011. Remote Sens. Lett. **4:** 764-773, doi:10.1080/2150704X.2013.796433.

Hu, C., L. Feng, R. F. Hardy and E. J. Hochberg. 2015. Spectral and spatial requirements of remote measurements of pelagic Sargassum macroalgae. Remote Sens. Environ. **167:** 229-246, doi://doi.org/10.1016/j.rse.2015.05.022.

Johnson, D., D. Ko, J. Franks S., P. Moreno and G. Sanchez-Rubio. 2013. The Sargassum Invasion of the Eastern Caribbean and Dynamics of the Equatorial North Atlantic. Proceed 65th GCFI. 102-103.

Laffoley, D., H. Roe, M. V. Angel, J. A. Ardron, N. R. Bates, I. L. Boyd, S. Brooke, K. N. Buck, C. A. Carlson, B. Causey, M. H. Conte, S. Christiansen, J. Cleary, J. Donnelly, S. A. Earle, R. Edwards, K. Gjerde, S. J. Giovannoni, S. Gulick and V. Vats. 2011. The protection and management of the Sargasso Sea: The golden floating rainforest of the Atlantic Ocean: Summary Science and Supporting Evidence Case. Sargasso Sea Alliance.

Lapointe, B. E. 1995. A comparison of nutrient-limited productivity in Sargassum natans from neritic vs. oceanic waters of the western North Atlantic Ocean. Limnol. Oceanogr. **40:** 625-633, doi:10.4319/lo.1995.40.3.0625.

Lomas, M. W., N. R. Bates, K. N. Buck and A. H. Knap. 2011. Notes on "Microbial Productivity of the Sargasso Sea and How it Compares to Elsewhere," and "The Role of the Sargasso Sea in Carbon Sequestration – Better than Carbon Neutral?". Sargasso Sea Alliance Report Series. **6:** 10.

Luckhurst, B., E. Prince, J. K Llopiz, D. Snodgrass and E. B Brothers. 2006. Evidence of blue marlin (Makaira nigricans) spawning in Bermuda waters and elevated mercury levels in large specimens. Bull. Mar. Sci. **79:** 691-704.

Manzella, S., J. Williams, B. Schroeder and W. Teas. 2011. Juvenile Head-Started Kemp's Ridleys Found in Floating Grass Mats. Marine Turtle Newsletter. **52:** 5-6.

Maurer, A., E. De Neef and S. Stapleton. 2015. Sargassum accumulation may spell trouble for nesting sea turtles. Front. Ecol. Environ. **13:** 394-395, doi:10.1890/1540-9295-13.7.394.

Parr, A. E. 1939. Quantitative observations on the pelagic sargassum vegetation of the western north Atlantic. Bingham Oceanographic Foundation.

Putman, N. F., G. J. Goni, L. J. Gramer, C. Hu, E. M. Johns, J. Trinanes and M. Wang. 2018. Simulating transport pathways of pelagic Sargassum from the Equatorial Atlantic into the Caribbean Sea. Prog. Oceanogr. **165:** 205-214, doi://doi.org/10.1016/j.pocean.2018.06.009.

Ryther, J. H. 1956. The Sargasso Sea. Sci. Am. 99-104.

Schell, J., D. Goodwin and A. Siuda. 2015. Recent Sargassum Inundation Events in the Caribbean: Shipboard Observations Reveal Dominance of a Previously Rare Form. Oceanography. **28:** 8-10, doi:10.5670/oceanog.2015.70.

Schwartz, F. J. 1998. Aggregations of Young Hatchling Loggerhead Sea Turtles in the Sargassum off North Carolina. Marine Turtle Newsletter. 9-10.

South Atlantic Fishery Management Council. 1998. Calico Scallop Fishery and Sargassum Habitat Fishery: Environmental Impact Statement. NOAA.

South Atlantic Fishery Management Council. 2002. Fishery management plan for pelagic Sargassum habitat of the South Atlantic Region. NOAA.

Stoner, A. W. 1983. Pelagic Sargassum: Evidence for a major decrease in biomass. Deep Sea Research Part A. Oceanographic Research Papers. **30:** 469-474, doi://doi.org/10.1016/0198-0149(83)90079-1.

Wang, M. and C. Hu. 2016. Mapping and quantifying Sargassum distribution and coverage in the Central West Atlantic using MODIS observations. **183:** 350-367.

Wang, M., and C. Hu. 2017. Predicting Sargassum blooms in the Caribbean Sea from MODIS observations: Sargassum Bloom Prediction.

Wilson, L.,J., X. Weber, T. King, and C. Fraser. 2016. DNA Extraction Techniques for Genomic Analyses of Macroalgae, p. 363-386. *In* Anonymous Seaweed Phylogeography.

APPENDIX

Table 1. Cox3 touchdown polymerase chain reaction (PCR) protocol.

Step	Temperature	Duration (seconds)	Function
1	94°C	240	initial denaturation
2	94°C	60	denature
3	50°C	30	anneal
4	68°C	60	extension
5	*repeat Steps 2-4, 4 more times*		
6	94°C	60	denature
7	48°C	30	anneal
8	68°C	60	extension
9	*repeat Steps 6-8, 4 more times*		
10	94°C	60	denature
11	46°C	30	anneal
12	68°C	60	extension
13	*repeat Steps 10-12, 9 more times*		
14	94°C	60	denature
15	44°C	30	anneal
16	68°C	60	extension
17	*repeat Steps 14-16, 9 more times*		
18	94°C	60	denature
19	42°C	30	anneal
20	68°C	60	extension
21	*repeat Steps 18-20, 9 more times*		
22	68°C	420	final extension
23	4°C	3,600	cool down

Table 2. Nad6 touchdown polymerase chain reaction (PCR) protocol.

Step	Temperature	Duration (seconds)	Function
1	95°C	180	initial denaturation
2	95°C	45	denature
3	54°C	60	anneal
4	72°C	180	extension
5	*repeat Steps 2-4, 25 more times*		
6	72°C	600	final extension
7	4°C	3,600	cool down